Effects of etidronate on the Enpp1-/- mouse model of generalized arterial calcification of infancy

Effects of etidronate on the *Enpp1*$^{-/-}$ mouse model of generalized arterial calcification of infancy

CARMEN HUESA[1*], KATHERINE A. STAINES[1*], JOSE LUIS MILLÁN[2] and VICKY E. MacRAE[1]

[1]Roslin Institute and R(D)SVS, The University of Edinburgh, Edinburgh, UK;
[2]Sanford Children's Health Research Center, Sanford-Burnham Medical Research Institute, La Jolla, CA, USA

Received February 27, 2015; Accepted April 22, 2015

DOI: 10.3892/ijmm.2015.2212

Abstract. Generalized arterial calcification of infancy (GACI) is an autosomal recessive disorder of spontaneous infantile arterial and periarticular calcification which is attributed to mutations in the ectonucleotide pyrophosphatase/phosphodiesterase 1 (*Enpp1*) gene. Whilst the bisphosphonate, etidronate, is currently used off-label for the treatment for GACI, recent studies have highlighted its detrimental effects on bone mineralisation. In the present study, we used the *Enpp1*$^{-/-}$ mouse model of GACI to examine the effects of etidronate treatment (100 μg/kg), on vascular and skeletal calcification. Micro-computed tomography (μCT) analysis revealed a significant decrease in trabecular bone mass, as reflected by the decrease in trabecular bone volume/tissue volume (BV/TV; %), trabecular thickness, trabecular separation, trabecular number and pattern factor ($P<0.05$) in the *Enpp1*$^{-/-}$ mice in comparison to the wild-type (WT) mice. Mechanical testing revealed that in the WT mice, treatment with etidronate significantly improved work to fracture and increased work post-failure ($P<0.05$, in comparison to the vehicle-treated WT mice). This significant increase, however, was not observed in the *Enpp1*$^{-/-}$ mice. Treatment with etidronate had no effect on bone parameters in the WT mice; however, the *Enpp1*$^{-/-}$ mice displayed an increased structural model index (SMI; $P<0.05$). We used a recently developed 3D μCT protocol to reconstruct and quantify the extensive aortic calcification in *Enpp1*$^{-/-}$ mice in comparison to the WT mice. However, treatment with etidronate did not prevent *de novo* calcification, and did not arrest the progression of established calcification of the aorta.

Correspondence to: Dr Katherine A. Staines, Roslin Institute and R(D)SVS, The University of Edinburgh, Easter Bush, Midlothian, Edinburgh EH25 9RG, UK
E-mail: katherine.staines@roslin.ed.ac.uk

*Contributed equally

Key words: mineralization, vascular calcification, ectonucleotide pyrophosphatase/phosphodiesterase 1, etidronate, generalized arterial calcification of infancy

Introduction

Generalized arterial calcification of infancy (GACI) is an autosomal recessive disorder of spontaneous infantile arterial and periarticular calcification (1-3). This life-threatening disease is caused by loss-of-function mutations in the ectonucleotide pyrophosphatase/phosphodiesterase 1 (*ENPP1*) gene, a key regulator of biomineralisation and vascular calcification (4-8).

ENPP1 is a cell-surface glycoprotein enzyme that functions in synergy with the anklyosis protein (ANK) to respectively form and intracellularly channel inorganic pyrophosphate (PP_i), an inhibitor of hydroxyapatite formation, from nucleoside triphosphates (9-12). The extracellular concentration of PP_i is further influenced by tissue non-specific alkaline phosphatase (TNSALP), another cell-surface enzyme located on the cell membrane of osteoblasts and chondrocytes, as well as on the membranes of their matrix vesicles (MVs) (13). TNSALP exerts its effects by hydrolysing PP_i reducing the concentration of this mineralisation inhibitor and establishing a phosphate (Pi)/PP_i ratio permissive for the formation of hydroxyapatite crystals (14-17). Phosphatase, orphan 1 (PHOSPHO1) is another essential phosphatase, located within osteoblast- and chondrocyte-derived MVs with high phosphohydrolase activity toward phosphoethanolamine and phosphocholine (18-22), which contributes Pi for the initiation of skeletal mineralisation. Together, ENPP1, ANK, TNSALP and PHOSPHO1 control the Pi/PPi ratio conducive to physiological skeletal mineralisation. Thus, ENPP1 in GACI reduces extracellular PP_i levels and predisposes to ectopic calcification. This was further exemplified in a previous study of ours, in which we determined that vascular smooth muscle cells from mice deficient in *Enpp1* have increased TNSALP levels (23).

In naturally occurring mouse models, the link between defective *Enpp1* expression and altered mineralisation was initially demonstrated in 'tiptoe walking' (*ttw/ttw*) mice (24-28). These animals are homozygous for a G→T substitution resulting in the introduction of a stop codon in the NPP1 coding sequence. The subsequent truncated protein leads to the loss of a vital calcium binding domain and two putative glycosylation sites (25). The phenotype of this mouse includes the postnatal development of progressive ankylosing intervertebral and peripheral joint hyperostosis, as well as spontaneous arterial and articular cartilage calcification and increased vertebral cortical bone formation (24-28). Transgenic mice that are homozygous for a

disruption in exon 9 of the *Enpp1* gene (*Enpp1*$^{-/-}$ *mice*) exhibit abnormalities that are almost identical to those present in *ttw/ttw* mice (29). These include decreased levels of extracellular PP_i, with phenotypic characteristics, including significant alterations in bone mineralisation in long bones and calvariae, and pathological, severe peri-spinal soft tissue and arterial calcification (30-32).

Effective treatment for infants and young children with GACI is critical as without it, 85% of patients succumb to the disease within 6 months of age. First used off-label in the treatment of *Fibrodysplasia ossificans progressiva*, the 'first generation' bisphosphonate, etidronate (EHDP; ethane-1-hydroxy-1,1-diphosphonic acid, also known as 1-hydroxyethylidene-bisphosphonate) is an analogue of PP_i and has also been used in the treatment of GACI. Bisphosphonates are potent inhibitors of osteoclast activity, and are widely used in clinical practice to prevent the bone loss associated with conditions, such as Paget's disease, metastatic bone disease and osteoporosis (33). The inhibitory effects of bisphosphonates on osteoblast function have also been demonstrated (34-37).

In 2008, a retrospective observational analysis of 55 patients with GACI revealed survival beyond infancy with etidronate therapy (38) corroborated by a recent study highlighting that 15 out of 22 GACI survivors received etidronate (39). However, studies on uremic rats have suggested that the administration of etidronate may not be able to prevent arterial calcification without inhibiting bone formation (40). Furthermore, a recent case report has highlighted the profound inhibition of skeletal mineralisation with paradoxical joint calcifications following protracted etidronate therapy in a 7-year-old boy with GACI (41). Taken together, these findings have led us to herein assess the effects of etidronate on bone architecture and arterial calcification in the *Enpp1*$^{-/-}$ mouse model of GACI.

Materials and methods

Animals. Enpp1$^{-/-}$ and wild-type (WT) mice were generated and maintained as previously described (1,5,29,42). Male mice were administered etidronate at 100 μg/kg, intraperitoneally twice a week from 11 to 22 weeks of age. The dosage of etidronate used in this study was based on the dose reported in a previously study (43). Animals were administered saline as a placebo (vehicle treatment). All animals were weighed once a week. The animals were sacrificed at 22 weeks of age and the tissues were dissected for further analysis. All animal experiments were approved by The Roslin Institute's Animal Users Committee and the animals were maintained in accordance with the UK Home Office guidelines for the care and use of laboratory animals (PIL number DD 60/3828).

Preparation of tissue. The aortae and tibiae were dissected as previously described (5). The aortae were fixed in 10% neutral buffered formalin (NBF) for 48 h before being transferred to 70% ethanol. The tibiae were immediately frozen in distilled water pending analysis.

Micro-computed tomography (μCT) of the aortae. Prior to scanning, the aortae were immersed for a minimum period of time (10 min) in a macro-molecular iopamidol-based contrast agent (Niopam 300; Brako UK Ltd., High Wycombe, Buckinghamshire, UK) diluted 1:4 in water as previously described (44). To allow tissue differentiation, aortic luminae were filled with corn oil and the aortae were submersed in oil for the duration of the scan. Tissues were imaged using a Skyscan 1172 X-Ray Microtomograph (Bruker Daltonics, Brussels, Belgium). Sequential high-resolution scans were acquired using a rotation step of 0.3˚ with the averaging of 3 frames at each step, applying a 0.5-mm aluminium filter, with an X-ray source set at 60 kV and 167 μA, and with an isotropic voxel size of 7 μm. The scans were reconstructed using NRecon (Bruker Daltonics). Noise in the reconstructed images was reduced by applying a median filter (radius = 1). The region of interest was selected to be the aortic arch, 200 lices (1.4 mm) under the subclavian artery. Soft and calcified tissue was identified by thresholding using CTAn software (Bruker Daltonics).

μCT of the tibiae. High-resolution scans with an isotropic voxel size of 5 μm were acquired with a μCT system (60 kV, 0.5 mm aluminium filter, 0.6˚ rotation, Skyscan 1172; Bruker Daltonics). Scans were reconstructed using NRecon software (Bruker Daltonics). A 1,000-μm section of the metaphysis 250 μm off the reference plate was taken for analysis of the trabecular bone. The base of the growth plate was used as a standard reference point. A 250-μm metaphysis section of the mid-diaphysis, 1,500 μm below the reference plate, was scanned for the analysis of cortical structure. Data were analysed with CTAn software (Bruker Daltonics). The following parameters were analysed using CTAn software (Bruker Daltonics): percentage bone volume/trabecular bone volume (%BV/TV), trabecular number (Tb.N; /mm), trabecular patten factor (Tb.Pf), bone mineral density (BMD; g/cm^3), trabecular thickness (Tb.Th; mm), trabecular separation (Tb.Sp) and the structure model index (SMI) were evaluated. In the cortical bone, %BV/TV, BMD (g/cm^3), cortical thickness, cross-sectional area (mm^2), the percentage of closed pores and polar moment of inertia (mm^4) were evaluated.

Mechanical testing. Mechanical testing of the cortical bone was carried out using a Zwick materials testing machine (Zwick Armaturen GmbH, Ennepetal, Germany) and data were analysed as previously described (45). The span was fixed at 6.0 mm. The cross-head was lowered at 1 mm/min and data were recorded after every 0.1 mm change in deflection. Each bone was tested to fracture. Failure and fracture points were identified from the load-extension curve as the point of maximum load and where the load rapidly decreased to zero, respectively. The maximum stiffness was defined as the maximum gradient of the rising portion of this curve, and the yield point, the point at which the gradient reduced to 95% of this value. Both values were calculated from a polynomial curve fitted to the rising region of the load-extension curve.

Serum marker analysis. To determine differences in bone formation and resorption, plasma serum was collected from the mice at 22 weeks of age. A sandwich ELISA P1NP (IDS Ltd., Boldons, UK) and a C-terminal telopoptide of type I collagen (CTx) ELISA kit (RatLaps™; IDS) were used respectively, and analyses were performed according to the manufacturer's instructions.

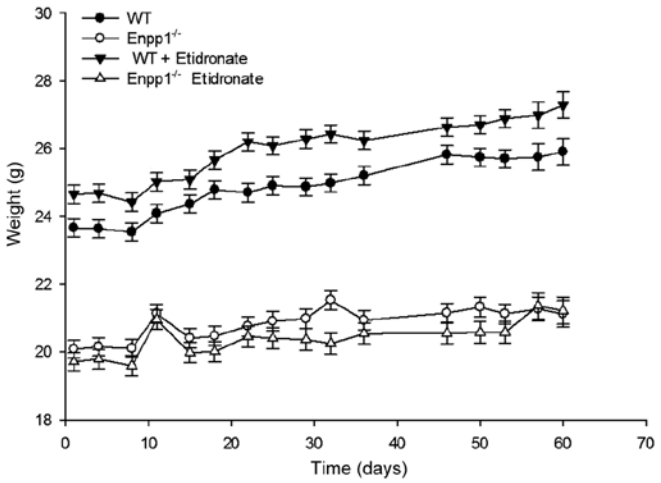

Figure 1. Body weight of 11-week-old male *Enpp1*$^{-/-}$ and wild-type (WT) mice taken for 60 days from the day of administration of etidronate (day 0). Data are expressed as the means ± SEM.

Statistical analysis. General linear model analysis, the Student's t-test, the Mann-Whitney non-parametric test and Pearson's correlation anlaysis were used to assess the data where appropriate. All data are expressed as the means ± SEM. Statistical analysis was performed using SPSS (IBM Software, New York, NY, USA). A value of P<0.05 was considered to indicate a statistically significant difference.

Results

Enpp1$^{-/-}$ *mouse growth phenotype*. In initial experiments, we examined whether the treatment of *Enpp1*$^{-/-}$ and WT mice with 100 μg/kg etidronate affects their growth. In accordance with our previous study, the *Enpp1*$^{-/-}$ mice exhibited a reduced growth in comparison to the WT mice (18.4% smaller than the age-matched WT controls; P<0.05) (5). Intraperitoneal injections of etidronate had no effect on the total body weight of the WT mice, nor the *Enpp1*$^{-/-}$ mice in comparison to the respective vehicle-treated mice (Fig. 1). Notably, the *Enpp1*$^{-/-}$ mice appeared to lose weight from approximately 12 weeks of age, which may be a consequence of their limited movement due to excessive joint calcification (Fig. 1) (1,5).

Aortic calcification. We have previously demonstrated that *Enpp1*$^{-/-}$ mice exhibit arterial calcification from 11 weeks of age (31). In this study, we employed our recently developed three-dimensional (3D) μCT protocol (44) for the quantification of aortic calcification to examine the effects of treatment with etidronate on mice lacking *Enpp1*. As expected, the *Enpp1*$^{-/-}$ mice exhibited extensive aortic calcification in comparison to the WT mice at 22 weeks of age (Fig. 2B). However, treatment with etidronate did not prevent *de novo* calcification, and did not arrest the progression of established calcification of the aorta in these mice (Fig. 2).

μCT analysis of bone microarchitecture. *Enpp1*$^{-/-}$ mice have previously been reported to display reduced mineral content in bone, with a reduction in bone volume fraction and trabecular thickness (5). The present study extended these observations by fully examining the effects of the administration of etidronate on the bone phenotype of *Enpp1*$^{-/-}$ mice. μCT analysis of the tibiae from *Enpp1*$^{-/-}$ mice in comparison to those from WT mice (both vehicle-treated) at 22 weeks of age revealed a significant decrease in trabecular bone mass, as reflected by a decrease in %BV/TV, trabecular thickness and trabecular number (P<0.05; Table I). Moreover, we observed a significant decrease in cortical parameters in the tibiae of the 22-week-old *Enpp1*$^{-/-}$

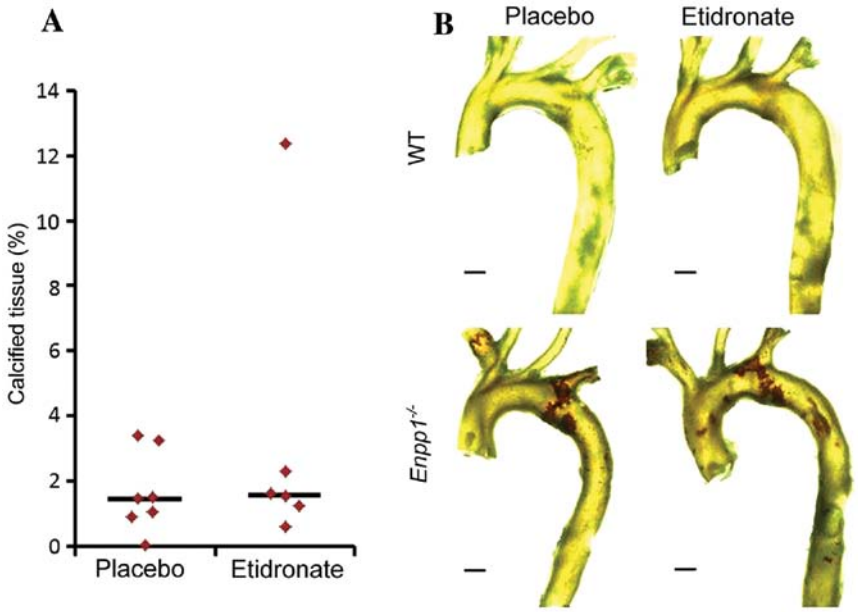

Figure 2. (A) Quantification (% of calcification) of calcium deposition in the aortae of 22-week-old *Enpp1*$^{-/-}$ mice. A standardised region of calcium deposition (400 slices from the subclavian artery) was selected and revealed no significant differences between the placebo (vehicle; saline)- and etidronate-treated groups. (B) Three-dimensional volumetric reconstructions of aortae from 22-week-old wild-type (WT) placebo-treated, WT etidronate-treated, *Enpp1*$^{-/-}$ placebo-treated, and *Enpp1*$^{-/-}$ etidronate-treated mice. Calcification is indicated by brown colouring. Bar represents 0.5 mm.

Table I. μCT analysis of trabecular bone in male placebo (vehicle)- and etidronate-treated *Enpp1*$^{-/-}$ and WT mice.

	WT		*Enpp1*$^{-/-}$	
	Placebo	Etidronate	Placebo	Etidronate
BV/TV (%)	8.79±1.59	8.75±1.79	3.39±1.06[a,e]	4.63±1.57[a,e]
BMD (g/cm^3)	0.139±0.021	0.13±0.024	0.042±0.020[a,e]	0.062±0.025[a,e]
Tb.Th (μm)	60.62±4.31	57.34±8.34	48.35±3.08[a,e]	47.99±3.54[a,d]
Tb.Sp (μm)	298.24±12.68	290.47±26.56	363.66±48.07[a,d]	319.66±48.44[b,c]
Tb.N	0.00146±0.00023	0.0015±0.00029	0.00070±0.00024[a,e]	0.00097±0.00034[a,e]
Tb.Pf	0.027±0.0026	0.026±0.0033	0.042±0.0036[a,e]	0.0392±0.0053[a,e]
SMI	2.48±0.11	2.33±0.23	2.78±0.093[a,d]	2.69±0.22[a,e]
DA	2.30±0.19	2.08±0.15	2.42±0.28	2.39±0.31[a,c]

Results are expressed as the means ± SEM. [a]Significant difference compared to wild-type (WT) mice; [b]significant difference compared to placebo-treated mice. [c]P<0.05; [d]P<0.01; [e]P<0.001. μCT, micro-computed tomography; BV/TV, bone volume/trabecular bone volume; BMD, bone mineral density; Tb.Th, trabecular thickness; Tb.Sp, trabecular separation; Tb.N, trabecular number; Tb.Pf, trabecular patten factor; SMI, structure model index; DA, degree of anisotropy.

Table II. μCT analysis of cortical bone in male placebo (vehicle)- and etidronate-treated *Enpp1*$^{-/-}$ and WT mice.

	WT		*Enpp1*$^{-/-}$	
	Placebo	Etidronate	Placebo	Etidronate
Co.BMD (g/cm^3)	1.18±0.018	1.18±0.020	1.20±0.024	1.20±0.011[a]
Co.Po (%)	53.27±7.26	54.79±5.64	61.75±3.71[a,c]	63.11±4.85[a,c]
Co.Th (μm)	197.90±1.91	195.64±3.84	175.98±5.96[a,d]	169.86±15.92[a,d]
Co.Area (μm^2)	5.14E+06±5.57E+05	5.09E+06±3.72E+05	4.47E+06±4.2E+05[a,e]	4.17E+06±4.3E+05[a,e]

Results are expressed as the means ± SEM. [a]Significant difference compared to wild-type (WT) mice; [b]significant difference compared to placebo-treated mice. [c]P<0.05; [d]P<0.01; [e]P<0.001. μCT, micro-computed tomography; cortical bone mineral density; Co.BMD, cortical bone mineral density; Co.Po; cortical porosity; Co.Th, cortical thickness; Co.Area, cortical area.

mice in comparison to the age-matched WT mice, except for cortical porosity (P<0.05; Table II). Treatment with etidronate had no significant effect on cortical or trabecular bone parameters in the WT mice (Tables I and II). In the *Enpp1*$^{-/-}$ mice, treatment with etidronate resulted in an increase in trabecular number and %BV/TV, as reflected by the significant decrease in trabecular separation (P<0.05, in comparison to the vehicle-treated *Enpp1*$^{-/-}$ mice) (Table I). The *Enpp1*$^{-/-}$ mice treated with etidronate did show a significant decrease in SMI [quantification of the plate- or rod-like geometry of trabecular structures, as previously described (46)] compared to the vehicle-treated *Enpp1*$^{-/-}$ mice (P<0.05; Table I).

Mechanical testing. The changes in bone geometry observed as a result of treatment with etidronate in the *Enpp1*$^{-/-}$ mice are likely to alter the biomechanical properties of long bones. In order to examine this hypothesis, we carried out 3-point bending analysis of the tibiae. Mechanical testing revealed a significant decrease in all mechanical parameters examined (stiffness, load at failure, work to failure, load at fracture, work to fracture, and yield) except work post-failure, in the *Enpp1*$^{-/-}$ mice compared to the WT mice at 22 weeks of age (Table III; P<0.05), reflecting reduced bone strength and stiffness as we have previously reported (5). In the WT mice, treatment with 100 μg/kg etidronate significantly improved work to fracture and increased work post-failure (Table III; P<0.05, in comparison to the vehicle-treated WT mice); this suggests that more energy is required to fracture these etidronate-treated bones in comparison to the vehicle-treated bones. This significant increase, however, was not observed in the *Enpp1*$^{-/-}$mice treated with etidronate (Table III).

Plasma biochemical markers. The level of osteoblast and osteoclast activity was assessed by ELISA of serum taken from the etidronate-treated and vehicle-treated 22-week-old male *Enpp1*$^{-/-}$ and WT mice. The plasma concentrations of P1NP, a marker of bone formation, were unaltered in the *Enpp1*$^{-/-}$ and WT mice at 22 weeks of age (Fig. 3A). Moreover, no significant differences in bone formation were observed upon the administration of etidronate in the WT or *Enpp1*$^{-/-}$ mice (Fig. 3A). The plasma concentrations of CTx, a marker of bone resorption, were increased in the *Enpp1*$^{-/-}$ mice in comparison to the WT mice in

Table III. Measurements of tibia mechanical properties in male placebo (vehicle)- and etidronate-treated *Enpp1*$^{-/-}$ and WT mice.

	WT		*Enpp1*$^{-/-}$	
	Placebo	Etidronate	Placebo	Etidronate
Stiffness (N/mm)	44.56±7.08	48.82±23.43	22.42±7.19[a,d]	22.52±6.64[a,e]
Load at failure (N)	17.22±2.90	15.34±4.13	9.21±1.38[a,e]	8.89±1.84[a,e]
Work to failure (J)	0.0066±0.00066	0.0064±0.0019	0.0033±0.00081[a,e]	0.0035±0.00092[a,e]
Load at fracture (N)	1.72±0.29	1.53±0.41	0.92±0.14[a,e]	0.89±0.18[a,e]
Work to fracture (J)	0.0069±0.00087	0.0086±0.0019[b,c]	0.0038±0.0011[a,e]	0.0044±0.00082[a,e]
Work post-failure (J)	0.00037±0.00041	0.0023±0.0014[b,d]	0.00055±0.00082	0.00088±0.0012[a,c]
Yield (N)	14.41±3.95	12.97±4.42	6.96±1.45[a,e]	7.11±1.79[a,d]

Results are expressed as the means ± SEM. [a]Significant difference compared to wild-type (WT) mice [b]significant difference compared to placebo-treated mice; [c]P<0.05; [d]P<0.01; [e]P<0.001.

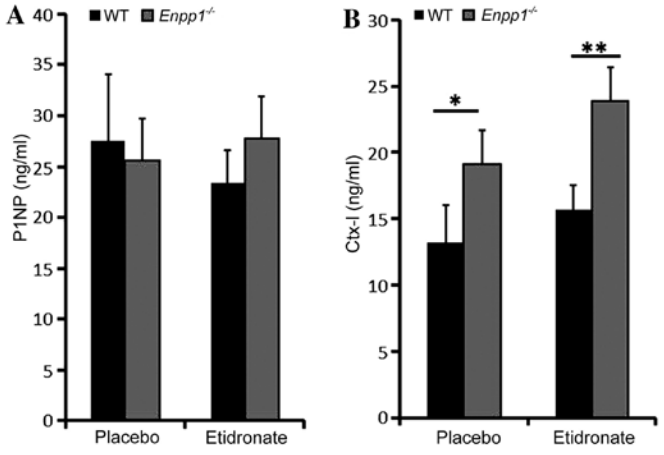

Figure 3. Serum marker analysis in *Enpp1*$^{-/-}$ and wild-type (WT) mice. (A) P1NP, a marker of bone formation; (B) CTx (RatLaps™), a marker of bone resorption. Results are expressed as the means ± SEM. *P<0.05; **P<0.01.

both the etidronate- and vehicle-treated mice (P<0.05; Fig. 3B). This is in concordance with our previous observation of this marker in *Enpp1*$^{-/-}$ mice (5). However, there were no significant differences observed between the etidronate- and vehicle-treated mice in either parameter (Fig. 3).

Discussion

Studies have associated treatment with bisphosphonates, chiefly etidronate, with improved survival in patients with GACI, an autosomal recessive disorder of spontaneous infantile arterial and periarticular calcification which is attributed to mutations in the *ENPP1* gene (38). Animal models have proven to be key to the understanding of pathological ectopic mineralisation (4,47). In particular, the *Enpp1*$^{-/-}$ mouse is of particular importance in advancing our understanding of GACI. Thus, the present study was undertaken to determine the effects of etidronate on *Enpp1*$^{-/-}$ mice.

Our data confirm and extend those of our previous study (5), demonstrating that tibiae from *Enpp1*$^{-/-}$ mice have a reduced trabecular bone mass and cortical thickness in comparison to WT mice, which explains the altered bone mechanical properties noted in the present study. This, therefore, is consistent with the depletion of NPP1 activity reducing extracellular PP_i to abnormally low levels, resulting in insufficient PP_i a substrate for TNAP to generate P_i for normal mineral formation. In the present study, we also used our novel 3D μCT protocol to provide evidence of the severe hypermineralisation of the arteries in *Enpp1*$^{-/-}$ mice, consistent with reduced extracellular PP_i levels predisposing the vascular system to ectopic calcification.

Bisphosphonates are typically prescribed for the treatment of osteoporosis and to reduce fracture risk, preventing bone loss primarily by the inhibition of osteoclast function (33). However, there is evidence to suggest that bisphosphonates impair the anabolic response of bone to parathyroid hormone (48), inhibiting osteoblast function and suppressing bone formation (34-37). Furthermore, the hydrolysis-resistant P-C-P motif of bisphosphonates resembles the TNSALP susceptible core of PP_i, (49) permitting bisphosphonates to impair calcium phosphate crystallisation (50). First used off-label in the treatment of *Fibrodysplasia ossificans progressiva*, the 'first generation' bisphosphonate, etidronate, is an analogue of PP_i, and whilst it is currently being investigated as a treatment for GACI, a number of studies have highlighted a number of detrimental effects with this approach, including the development of rickets or osteomalacia during the protracted administration of etidronate (40,41,51-56).

In this study, to clarify the effects of bisphosphonates on GACI, we treated WT and *Enpp1*$^{-/-}$ mice with 100 μg/kg etidronate. In the WT mice, treatment with etidronate had no effect on cortical or trabecular parameters as determined by μCT analysis. Despite this, treatment with etidronate significantly improved work to fracture and increased work post-failure, thus suggesting that more energy is required to fracture these bones in comparison to the vehicle-treated bones. The assessment of bone architecture in *Enpp1*$^{-/-}$ mice treated with etidronate revealed a significant decrease in SMI, a method for the determination of the plate- or rod-like geometry of trabecular structures. This change in bone geometry did not, however,

affect the bone mechanical properties. Consistent with this, the assessment of plasma markers of bone formation and resorption revealed that this dosage of etidronate did not significantly affect the bone remodelling process in the *Enpp1*$^{-/-}$ mice, nor in WT mice. These findings add further support to those of a recent *in vivo* study using mice, which also reported no effects of the administration of etidronate on bone resorption (57). Furthermore, the anti-resorptive effects of alendronate, risedronate and minodronate were revealed to be 1,000-, 3,300- and 10,000-fold greater than those of etidronate, respectively (57).

Surprisingly, and in contrast to previous data on rats with experimental renal failure (40), treatment with etidronate did not prevent *de novo* calcification, and did not arrest the progression of established calcification of the aorta in our *Enpp1*$^{-/-}$ mice. Taken together, these data suggest that the skeleton here is displaying an expected response to etidronate treatment, but this is not yet toxic to aortic calcification.

The mild effects of etidronate observed in this study may be explained by the dosage used, the frequency of administration and/or species differences. Future studies may aim to investigate a higher dosage and/or daily administration of etidronate, as previously it has been shown that high doses of etidronate significantly reduce mineralisation (58). Furthermore, in the present study, treatment of the mice commenced when the mice were 11 weeks of age, the point at which calcification is observed in this model (5). However, this initiation of treatment may have been too late to resolve underlying, pre-existing calcifications and additional investigation into this would allow further conclusions to be drawn.

In conclusion, despite the changes in bone microarchitecture, we did not observe an inhibition of aortic calcification or bone formation in the *Enpp1*$^{-/-}$ mice treated with etidronate. Additional studies are, therefore, required to fully determine whether etidronate is the most appropriate therapy for the treatment of GACI.

Acknowledgements

The present study was supported by an Institute Strategic Programme Grant and Institute Career Path Fellowship funding from the Biotechnology and Biological Sciences Research Council (BBSRC) (BB/F023928/1).

References

1. Rutsch F, Ruf N, Vaingankar S, Toliat MR, Suk A, Höhne W, Schauer G, Lehmann M, Roscioli T, Schnabel D, *et al*: Mutations in ENPP1 are associated with 'idiopathic' infantile arterial calcification. Nat Genet 34: 379-381, 2003.
2. Rutsch F, Vaingankar S, Johnson K, Goldfine I, Maddux B, Schauerte P, Kalhoff H, Sano K, Boisvert WA, Superti-Furga A, *et al*: PC-1 nucleoside triphosphate pyrophosphohydrolase deficiency in idiopathic infantile arterial calcification. Am J Pathol 158: 543-554, 2001.
3. Nitschke Y and Rutsch F: Modulators of networks: Molecular targets of arterial calcification identified in man and mice. Curr Pharm Des 20: 5839-5852, 2014.
4. Mackenzie NC, Huesa C, Rutsch F and MacRae VE: New insights into NPP1 function: Lessons from clinical and animal studies. Bone 51: 961-968, 2012.
5. Mackenzie NC, Zhu D, Milne EM, van 't Hof R, Martin A, Darryl Quarles L, Millán JL, Farquharson C and MacRae VE: Altered bone development and an increase in FGF-23 expression in *Enpp1*$^{-/-}$ mice. PLoS One 7: e32177, 2012.
6. Apschner A, Huitema LF, Ponsioen B, Peterson-Maduro J and Schulte-Merker S: Zebrafish enpp1 mutants exhibit pathological mineralization, mimicking features of generalized arterial calcification of infancy (GACI) and pseudoxanthoma elasticum (PXE). Dis Model Mech 7: 811-822, 2014.
7. Hajjawi MO, MacRae VE, Huesa C, Boyde A, Millán JL, Arnett TR and Orriss IR: Mineralisation of collagen rich soft tissues and osteocyte lacunae in *Enpp1*$^{-/-}$ mice. Bone 69: 139-147, 2014.
8. Li Q, Guo H, Chou DW, Berndt A, Sundberg JP and Uitto J: Mutant Enpp1asj mice as a model for generalized arterial calcification of infancy. Dis Model Mech 6: 1227-1235, 2013.
9. Hakim FT, Cranley R, Brown KS, Eanes ED, Harne L and Oppenheim JJ: Hereditary joint disorder in progressive ankylosis (ank/ank) mice. I. Association of calcium hydroxyapatite deposition with inflammatory arthropathy. Arthritis Rheum 27: 1411-1420, 1984.
10. Terkeltaub R, Rosenbach M, Fong F and Goding J: Causal link between nucleotide pyrophosphohydrolase overactivity and increased intracellular inorganic pyrophosphate generation demonstrated by transfection of cultured fibroblasts and osteoblasts with plasma cell membrane glycoprotein-1. Relevance to calcium pyrophosphate dihydrate deposition disease. Arthritis Rheum 37: 934-941, 1994.
11. Addison WN, Azari F, Sørensen ES, Kaartinen MT and McKee MD: Pyrophosphate inhibits mineralization of osteoblast cultures by binding to mineral, up-regulating osteopontin, and inhibiting alkaline phosphatase activity. J Biol Chem 282: 15872-15883, 2007.
12. Staines KA, MacRae VE and Farquharson C: The importance of the SIBLING family of proteins on skeletal mineralisation and bone remodelling. J Endocrinol 214: 241-255, 2012.
13. Anderson HC: Molecular biology of matrix vesicles. Clin Orthop Relat Res (314): 266-280, 1995.
14. Moss DW, Eaton RH, Smith JK and Whitby LG: Association of inorganic-pyrophosphatase activity with human alkaline-phosphatase preparations. Biochem J 102: 53-57, 1967.
15. Majeska RJ and Wuthier RE: Studies on matrix vesicles isolated from chick epiphyseal cartilage. Association of pyrophosphatase and ATPase activities with alkaline phosphatase. Biochim Biophys Acta 391: 51-60, 1975.
16. Hessle L, Johnson KA, Anderson HC, Narisawa S, Sali A, Goding JW, Terkeltaub R and Millan JL: Tissue-nonspecific alkaline phosphatase and plasma cell membrane glycoprotein-1 are central antagonistic regulators of bone mineralization. Proc Natl Acad Sci USA 99: 9445-9449, 2002.
17. Murshed M, Schinke T, McKee MD and Karsenty G: Extracellular matrix mineralization is regulated locally; different roles of two gla-containing proteins. J Cell Biol 165: 625-630, 2004.
18. Macrae VE, Davey MG, McTeir L, Narisawa S, Yadav MC, Millan JL and Farquharson C: Inhibition of PHOSPHO1 activity results in impaired skeletal mineralization during limb development of the chick. Bone 46: 1146-1155, 2010.
19. Roberts S, Narisawa S, Harmey D, Millán JL and Farquharson C: Functional involvement of PHOSPHO1 in matrix vesicle-mediated skeletal mineralization. J Bone Miner Res 22: 617-627, 2007.
20. Roberts SJ, Owen HC and Farquharson C: Identification of a novel splice variant of the haloacid dehalogenase: PHOSPHO1. Biochem Biophys Res Commun 371: 872-876, 2008.
21. Stewart AJ, Roberts SJ, Seawright E, Davey MG, Fleming RH and Farquharson C: The presence of PHOSPHO1 in matrix vesicles and its developmental expression prior to skeletal mineralization. Bone 39: 1000-1007, 2006.
22. Yadav MC, Simão AM, Narisawa S, Huesa C, McKee MD, Farquharson C and Millán JL: Loss of skeletal mineralization by the simultaneous ablation of PHOSPHO1 and alkaline phosphatase function: A unified model of the mechanisms of initiation of skeletal calcification. J Bone Miner Res 26: 286-297, 2011.
23. Narisawa S, Harmey D, Yadav MC, O'Neill WC, Hoylaerts MF and Millán JL: Novel inhibitors of alkaline phosphatase suppress vascular smooth muscle cell calcification. J Bone Miner Res 22: 1700-1710, 2007.
24. Sakamoto M, Hosoda Y, Kojimahara K, Yamazaki T and Yoshimura Y: Arthritis and ankylosis in twy mice with hereditary multiple osteochondral lesions: With special reference to calcium deposition. Pathol Int 44: 420-427, 1994.
25. Okawa A, Goto S and Moriya H: Calcitonin simultaneously regulates both periosteal hyperostosis and trabecular osteopenia in the spinal hyperostotic mouse (twy/twy) in vivo. Calcif Tissue Int 64: 239-247, 1999.

26. Okawa A, Nakamura I, Goto S, Moriya H, Nakamura Y and Ikegawa S: Mutation in Npps in a mouse model of ossification of the posterior longitudinal ligament of the spine. Nat Genet 19: 271-273, 1998.
27. Baba H, Furusawa N, Fukuda M, Maezawa Y, Imura S, Kawahara N, Nakahashi K and Tomita K: Potential role of streptozotocin in enhancing ossification of the posterior longitudinal ligament of the cervical spine in the hereditary spinal hyperostotic mouse (twy/twy). Eur J Histochem 41: 191-202, 1997.
28. Furusawa N, Baba H, Imura S and Fukuda M: Characteristics and mechanism of the ossification of posterior longitudinal ligament in the tip-toe walking Yoshimura (twy) mouse. Eur J Histochem 40: 199-210, 1996.
29. Sali A, Favaloro J, Terkeltaub R and Goding J: Germline deletion of the nucleoside triphosphate pyrophosphohydrolase (NTPPPH) plasma cell membrane glycoprotein-1 (PC-1) produces abnormal calcification of periarticular tissues. In: Ecto-ATPases and Related Ectoenzymes. Vanduffel L and Lemmems R (eds). Shaker Publishing BV, Maastricht, The Netherlands, pp267-282, 1999.
30. Harmey D, Hessle L, Narisawa S, Johnson KA, Terkeltaub R and Millán JL: Concerted regulation of inorganic pyrophosphate and osteopontin by akp2, enpp1, and ank: An integrated model of the pathogenesis of mineralization disorders. Am J Pathol 164: 1199-1209, 2004.
31. Anderson HC, Harmey D, Camacho NP, Garimella R, Sipe JB, Tague S, Bi X, Johnson K, Terkeltaub R and Millán JL: Sustained osteomalacia of long bones despite major improvement in other hypophosphatasia-related mineral deficits in tissue nonspecific alkaline phosphatase/nucleotide pyrophosphatase phosphodiesterase 1 double-deficient mice. Am J Pathol 166: 1711-1720, 2005.
32. Johnson K, Goding J, Van Etten D, Sali A, Hu SI, Farley D, Krug H, Hessle L, Millán JL and Terkeltaub R: Linked deficiencies in extracellular PP_i and osteopontin mediate pathologic calcification associated with defective PC-1 and ANK expression. J Bone Miner Res 18: 994-1004, 2003.
33. Russell RG: Bisphosphonates: From bench to bedside. Ann NY Acad Sci 1068: 367-401, 2006.
34. Orriss IR, Key ML, Colston KW and Arnett TR: Inhibition of osteoblast function in vitro by aminobisphosphonates. J Cell Biochem 106: 109-118, 2009.
35. Idris AI, Rojas J, Greig IR, Van't Hof RJ and Ralston SH: Aminobisphosphonates cause osteoblast apoptosis and inhibit bone nodule formation in vitro. Calcif Tissue Int 82: 191-201, 2008.
36. Iwata K, Li J, Follet H, Phipps RJ and Burr DB: Bisphosphonates suppress periosteal osteoblast activity independently of resorption in rat femur and tibia. Bone 39: 1053-1058, 2006.
37. Tobias JH, Chow JW and Chambers TJ: 3-Amino-1-hydroxypropylidine-1-bisphosphonate (AHPrBP) suppresses not only the induction of new, but also the persistence of existing bone-forming surfaces in rat cancellous bone. Bone 14: 619-623, 1993.
38. Rutsch F, Böyer P, Nitschke Y, Ruf N, Lorenz-Depierieux B, Wittkampf T, Weissen-Plenz G, Fischer RJ, Mughal Z, Gregory JW, *et al*; GACI Study Group: Hypophosphatemia, hyperphosphaturia, and bisphosphonate treatment are associated with survival beyond infancy in generalized arterial calcification of infancy. Circ Cardiovasc Genet 1: 133-140, 2008.
39. Chong CR and Hutchins GM: Idiopathic infantile arterial calcification: The spectrum of clinical presentations. Pediatr Dev Pathol 11: 405-415, 2008.
40. Lomashvili KA, Monier-Faugere MC, Wang X, Malluche HH and O'Neill WC: Effect of bisphosphonates on vascular calcification and bone metabolism in experimental renal failure. Kidney Int 75: 617-625, 2009.
41. Otero JE, Gottesman GS, McAlister WH, Mumm S, Madson KL, Kiffer-Moreira T, Sheen C, Millán JL, Ericson KL and Whyte MP: Severe skeletal toxicity from protracted etidronate therapy for generalized arterial calcification of infancy. J Bone Miner Res 28: 419-430, 2013.
42. Huesa C, Zhu D, Glover JD, Ferron M, Karsenty G, Milne EM, Millan JL, Ahmed SF, Farquharson C, Morton NM, *et al*: Deficiency of the bone mineralization inhibitor NPP1 protects mice against obesity and diabetes. Dis Model Mech 7: 1341-1350, 2014.
43. Sugiyama T, Meakin LB, Galea GL, Jackson BF, Lanyon LE, Ebetino FH, Russell RG and Price JS: Risedronate does not reduce mechanical loading-related increases in cortical and trabecular bone mass in mice. Bone 49: 133-139, 2011.
44. Huesa C, Millán JL, van 't Hof RJ and MacRae VE: A new method for the quantification of aortic calcification by three-dimensional micro-computed tomography. Int J Mol Med 32: 1047-1050, 2013.
45. Huesa C, Yadav MC, Finnilä MA, Goodyear SR, Robins SP, Tanner KE, Aspden RM, Millán JL and Farquharson C: PHOSPHO1 is essential for mechanically competent mineralization and the avoidance of spontaneous fractures. Bone 48: 1066-1074, 2011.
46. Hildebrand T and Ruegsegger P: A new method for the model-independent assessment of thickness in three-dimensional images. J Microscopy (Oxford) 185: 67-75, 1997.
47. Li Q and Uitto J: Mineralization/anti-mineralization networks in the skin and vascular connective tissues. Am J Pathol 183: 10-18, 2013.
48. Black DM, Greenspan SL, Ensrud KE, Palermo L, McGowan JA, Lang TF, Garnero P, Bouxsein ML, Bilezikian JP and Rosen CJ; PaTH Study Investigators: The effects of parathyroid hormone and alendronate alone or in combination in postmenopausal osteoporosis. N Engl J Med 349: 1207-1215, 2003.
49. Fleisch H, Russell RG and Straumann F: Effect of pyrophosphate on hydroxyapatite and its implications in calcium homeostasis. Nature 212: 901-903, 1966.
50. Felix R, Herrmann W and Fleisch H: Stimulation of precipitation of calcium phosphate by matrix vesicles. Biochem J 170: 681-691, 1978.
51. Thiaville A, Smets A, Clercx A and Perlmutter N: Idiopathic infantile arterial calcification: A surviving patient with renal artery stenosis. Pediatr Radiol 24: 506-508, 1994.
52. Van Dyck M, Proesmans W, Van Hollebeke E, Marchal G and Moerman P: Idiopathic infantile arterial calcification with cardiac, renal and central nervous system involvement. Eur J Pediatr 148: 374-377, 1989.
53. Thomas T, Lafage MH and Alexandre C: Atypical osteomalacia after 2 year etidronate intermittent cyclic administration in osteoporosis. J Rheumatol 22: 2183-2185, 1995.
54. Silverman SL, Hurvitz EA, Nelson VS and Chiodo A: Rachitic syndrome after disodium etidronate therapy in an adolescent. Arch Phys Med Rehabil 75: 118-120, 1994.
55. Russell RG, Smith R, Preston C, Walton RJ and Woods CG: Diphosphonates in Paget's disease. Lancet 1: 894-898, 1974.
56. Smith R, Russell RG and Woods CG: Myositis ossificans progressiva. Clinical features of eight patients and their response to treatment. J Bone Joint Surg Br 58: 48-57, 1976.
57. Kim S, Seiryu M, Okada S, Kuroishi T, Takano-Yamamoto T, Sugawara S and Endo Y: Analgesic effects of the non-nitrogen-containing bisphosphonates etidronate and clodronate, independent of anti-resorptive effects on bone. Eur J Pharmacol 699: 14-22, 2013.
58. Li Q, Sundberg JP, Levine MA, Terry SF and Uitto J: The effects of bisphosphonates on ectopic soft tissue mineralization caused by mutations in the *ABCC6* gene. Cell Cycle 14: 1082-1089, 2015.